Applied Mathematics & Information Sciences **3**(3) (2009), 273–299
– An International Journal

Schrödinger Cats in Double Well Bose Condensates: Modeling Their Collapse and Detection via Quantum State Diffusion

William P. Reinhardt[1], Cynthia A. Stanich[1], and Cory D. Schillaci[2]

[1]Department of Chemistry, Campus Box 351700, University of Washington

Seattle, WA 98105-1700, U.S.A.

E-mail addresses: rein@chem.washington.edu (WPR) c.a.stanich@gmail.com (CAS)

[2]Department of Physics, Campus Box 351560, University of Washington

Seattle, WA 98105-1560, U.S.A.

E-mail address: cdschillaci@gmail.com

Can macroscopic quantum superposition states (or highly entangled number states) be *observed directly*? Specifically, can phase contrast imaging be applied to observe a superposition state with essentially "all" of the atoms in a gaseous double well BEC being simultaneously in both wells at the same time? That is we are looking to image states of the type $|N,0> + |0,N>$ where $|L,R>$ denotes L particles in the Left well and R in the Right. We will happily settle for states of the form $|N-n,n> + |n,N-n>$, with $n << N$, these being less ephemeral. Earlier work in our group, Perry, Reinhardt and Kahn, has shown that such highly entangled number states may be generated by appropriate *phase engineering*, just as in the case of the phase engineering of solitons in single well BECs. Experimentalists have been hesitant to attempt to create such states in fear that definitive observations cannot be carried out. There have also been suggestions that "Nature" will prevent such superpositions from existing for N too large ... and thus there are also basic issues in quantum theory which may prevent the formation and detection of such states. In the present progress report we begin an investigation of calculating the lifetimes of such entangled states in the presence of both observation and spontaneous decay both of which perturb, and eventually destroy, the entanglement under investigation via quantum back-action. Quantum State Diffusion (QSD) provides a useful computational tool in addressing such questions, and we present the initial results of exploring this novel use of QSD.

Keywords: Schrödinger Cats, Gaseous Bose-Einstein Condensates, BECs in Double Wells, Quantum State Diffusion (QSD), Modeling Detection of Number Entan-

This work has been supported, in part, by NSF Grant PHYS 0703278, WPR, PI; by the awarding of a University of Washington Mary Gates Research Scholarship to CDS; and by support for CAS from the Department of Chemistry and the College of Arts and Sciences.

gled States via Quantum State Diffusion, Macroscopic Quantum Superposition States, Number Entangled States, Non-destructive Imaging of BECs.

1 Introduction

"Can Quantum-Mechanical Description of Physical Reality Be Considered Complete?" A. Einstein, B. Poldoski, and N. Rosen, The Physical Review, 1935.

It is a commonplace that "no one understands" quantum mechanics. In a Young's double slit experiment, individual electrons [39] seemingly act like "waves" in a superposition state, passing though both slits simultaneously and thus producing the well known double slit interference patterns. Yet they may also be, in fact can only be, counted as discrete particles which arrive, one at a time, at the photo-plate detector with definite energies, locations, and other familiar properties of particles. Bohr referred to this as complementarity. Einstein insisted that such a theory was, while perhaps not wrong, at least incomplete, as discussed and exemplified in the famous "EPR" paper [32]. See also Bohr's response [7]. Bell [5, chapters 10, 16] gives an illuminating comparison of Einstein's and Bohr's views regarding this *situation*. In a paper entitled "The current *situation* in quantum theory," also a response to EPR, Schrödinger introduced his infamous Cat to argue that one could never see an elementary particle in a superposition state. Such a particle, he argued, could not be simultaneously observed in both slits in an interference experiment or directly observed in a superposition of being "decayed and not decayed." Observation yields only one or the other possibility [36]. See also the useful English translations of these Schrödinger papers by Trimmer [40]. Thus, Schrödinger argued that the wave-function aspects of quantum theory are indeed a fiction. In agreement with Bohr, he also insisted that quantum mechanics was a statistically predictive theory, but one in which the underlying mathematics have no physical interpretation. At this point, it is useful to note that both the EPR and Schrödinger Cat papers involve what Schrödinger was the first to call *entanglement*, which will emerge to be the main topic of interest in the present paper. The development of quantum mechanics has been accompanied by parallel efforts to develop alternative formulations of the theory which make correct quantum predictions but also give rise to classical-like visualizations. These alternate theories would then provide the understanding *presumed to be missing* of what *really goes on* in quantum dynamics. Of course, there may or not be such *missing understanding* to begin with. See, for example, the development of the mixed classical and quantum theory by Bohm [6], and the overview essays of Bell [5], Leggett [18] and Omnes [26].

Another challenging aspect of quantum mechanics relates to the question: how does the familiar world of "classical dynamics" emerge from the quantum world? Ghirardi *et al.* [14], and Penrose [27], among others, have suggested that the familiar world we

see around us arises as quantum properties are "suppressed or quenched" beyond certain *masses or particle numbers*. This allows emergence of the classical world, in which interference effects seemingly vanish, because the Schrödinger equation is modified as physical systems grow in size. Others [26, 35], to cite representative overviews of a long running thema, argue that *decoherence*, namely the interaction of quantum systems with finite temperature classical systems (or even warm quantum systems), quenches quantum properties. This quenching again leads to the classical world in which we seem to live. The issue of the distinction between *the quantum system* and *its environment* "complicates" such discussions, to say the least.

At the same time, entanglement [32, 36] is, although among the strangest of quantum phenomena, the basis of quantum information processing, quantum encryption, and possibly quantum computation. See Neilson and Chuang for an overview of all three [25]. These new technologies simply take quantum mechanics at face value, utilizing its deepest mysteries to practical and commercial advantage.

Why quantum computation? As Feynman pointed out [10], quantum systems have no trouble time evolving themselves very efficiently, yet classical computers are very inefficient when they attempt to mimic quantum dynamics. The solution is to build special quantum systems, known as quantum computers, which emulate other quantum systems while hopefully performing other useful tasks as well. Quantum information processing and encryption have been experimentally realized and have begun to appear outside of optics and physics laboratories. A quantum encrypted cell phone might well be on the market in the near future, but it will not be cheap because encryption may well rely on entangled photon pairs from orbiting satellites! Precision time measurements, foundational to modern communications and the GPS system of Global navigation, are being upgraded with the help of entanglement as these words are being written. Thus the quantum and classical worlds are beginning to mix at a level of practicality and engineering well beyond that of the now common devices which exploit quantum properties for simple switches.

It has been tacitly assumed in the above that quantum systems consist of single, or small numbers of, elementary particles. Schrödinger considered the entanglement of a single atom with his "living" or "dead" cat to make the point that one would never observe the atom in a superposition state, otherwise we would also necessarily find the cat in a superposition state. He argued that, as no one has ever seen a cat in a superposition state, we should not imagine that we could do so for an atom. This is not the place to critique this argument on its own terms, as many would argue that even the above statement of the problem is rather simplistic [18, 26, 35]. After all, the cat is a warm classical system and has likely decohered, losing any initial quantum nature more quickly than any measurement can be made to detect that nature. See, for example, Omnes [26, Chapter 19].

Recently, however, free standing "large" quantum systems consisting of thousands or even millions of atoms, and showing full quantum coherences, have been created [2]. This

feat has subsequently been repeated in laboratories all over the world. These are the gaseous atomic Bose-Einstein condensates (BECs) [19, 20, 29, 30], which following their creation have been found to be fully coherent [4,37], subject to quantum "phase engineering" which can create quantum solitons [9, 33, 42], and to exhibit macroscopic and coherent quantum, Josephson-like tunneling [1]. It may certainly be argued that the rather earlier discoveries of super-fluidity and superconductivity, see for example [20,38], are also examples of "large" quantum systems. However, these latter types of macroscopic quantum behavior are "hidden" within the liquids or solids which contain them. These consist of elemental particles whose properties are not subject to experimental control, and thus offer far less opportunity for comprehensive study than the gaseous BECs. Through optical manipulations and trap trickery, the shapes, densities, number of independent species, and even the fundamental interparticle interactions in a gaseous condensate may be "tuned" almost at will. This allows their properties to be explored over a great range of physical situations [19, 20, 30], perhaps including macroscopic superposition states.

Will this possibility of macroscopic quantum systems in "superposition" lead to direct observation of quantum superposition for macroscopic states? Experiments in superconductors have shown "avoided" crossings of the energy levels of such macroscopic systems [13, 41], leading to the possible conclusion that a signature of macroscopic quantum superposition states has already been observed. However, it is likely that only a few of the elementary bosonic particles (bosonic Cooper pairs in the case of superconductivity [20]) are actually involved in such level-crossing observations, see Reinhardt and Perry [34]. Furthermore, we would like to actually *see*, visualize, or take a picture of such a state, which is simply not possible in a typical metallic superconductor; all of the quantum mechanical processes are hidden in the solid state matrix that supports it.

For gaseous BECs in magnetic traps, however, actual photographs of the quantum condensate have been taken from the time of the earliest experiments. For example, in observing the sloshing of a BEC of Rb atoms in a harmonic trap experimentalists have made an actual movie or "film" of the moving condensate [15]. The same is the case for the dynamics of solitons as seen in [9]. On the other hand, in these experiments the visualization of dynamics is created by a series of experiments made on identically prepared replicas of a time evolving condensate. Images are *photographed* at an appropriate sequence of times in the evolution of different condensates, and each replica condensate is destroyed in the process of being imaged. This follows from the fact that the atoms are observed through actual absorption of resonance radiation. This process knocks many of the atoms out of the BEC via momentum recoil and leaves any remaining condensate atoms decohered by heating from the exiting atoms.

Is there a way to image a BEC in a magnetic trap without destroying it? Ketterle *et al.* [3,17] have developed a form of non-destructive imaging and demonstrated that "many" images of the same condensate (rather than a series of identically prepared condensates)

may be taken, seemingly without destroying the condensate. This was at first called "quantum non-demolition imaging," but is actually a form of dark field microscopy [12] in that it detects slight differences in index of refraction via phase interferences of the probing photons. In such dark field imaging the light is off resonance to avoid absorption, but completely non-absorptive imaging is impossible. From arguments involving the optical theorem, or the Kramers-Krönig relations, it is easily concluded that the index of refraction is complex. The imaginary part leads to absorption (particle loss), and is non-zero even "far" off resonance, see Foot [11, Section 7.6] and the pedagogical discussion of Ketterle *et al.* [17]. Thus in the Ketterle [3] experiments a fraction of the atoms (on the order of 0.1%) are lost in each observation. In addition, the phase coherence of the condensate is disturbed in a manner complementary to the measurement of the local particle number [8]. Too many such "non-destructive" observations will decohere the condensate, essentially by imprinting a non-uniform phase which leads to local particle currents, just as in the case of soliton production [33]. These currents eventually heat the BEC, causing decoherence [8].

We are now, at last, in a position to state the purpose of the present progress report. Members of our group [23, 24] have demonstrated, within the frame work of the Bose-Hubbard model applied to a BEC in a double well, that highly number entangled states, also essentially Schrödinger Cat-type states, may be generated by phase engineering and described the subsequent dynamics of a ground state condensate. In such phase engineered states up to 95% of all particles are simultaneously in the left and right wells, and therefore in physically distinct locations. This is discussed in more detail in what follows. The question we are asking is simply: can an image show that *most of the atoms are simultaneously in both of the two wells*? That is, if we can make a macroscopic superposition state of large numbers of atoms in two places at the same time, can we produce a single image showing this to be the case? Said yet another way can we directly observe, using phase contrast photographic imaging, a macroscopic quantum superposition state of exactly the type that Schrödinger [36] suggested could not exist?

The outline of the progress report is a follows: to simulate observation of a quantum system, with the necessarily accompanying particle loss and the effects of particle detection back-action, we introduce Quantum State Diffusion (QSD) [28] as a numerical method for simulating actual quantum measurements. This results in a Brownian-type Monte-Carlo (i.e., statistical) method for simulation of an otherwise isolated quantum system as it interacts with a measuring apparatus and data are collected. Collection of such data also induces a "back action" on the original quantum system. However, unlike a destructive "all or nothing" measurement which collapses the wave function essentially instantly, the measurement(s) and subsequent back action are weak, as in a Ketterle [3] type dark field non-destructive imaging. Thus as information is *slowly* collected, the quantum system also feels the back action *slowly*, so we can explore the actual time scales on which data are taken. We then ask: can weak probing of a quantum system take place on a time scale such

that data may be taken before the combination of particle loss and quantum back-action destroys the macroscopic superposition we are attempting to observe? How does this possibility depend on the system size? The QSD method is briefly introduced in Section 2, and exemplified in Section 3 by the simple example of a quantum harmonic oscillator in a probing field which is also coupled to an external bath. This allows both decay and the effects of quantum back action to be seen. In Section 4 the method is applied to a superposition state of the single oscillator from Section 3. A simplified treatment, necessary to extend the method to large particle numbers, is introduced and found to perform reasonably well given its extreme simplicity. Number entangled states and their decay during observation are introduced in Section 5. Here we concentrate, not on a BEC in a double well, but on two distinct and uncoupled oscillators which can be prepared in a number entangled state. For example, we will consider states of the form $|M, N> + |N, M>$ which do not factor into a product of eigenstates of the single oscillators. Here $|M, N>$ denotes oscillator "1" in quantum state M, and oscillator "2" in state N. Full QSD calculations, even for just two such oscillators, become quickly time consuming as M, N increase, so we will let them go no larger than 6. As 6 is hardly the hundreds of thousands, or millions, of particles typical in laboratory BECs, the problem of carrying out full computations becomes the development of simple models which capture the essence of the full computations. We show that the decay of entangled states can be mimicked by an empirical QSD, which we call QSD2, involving only the two initial quantum states. Exploration of this approximation gives the central novel results of this report. Section 6 illustrates the utility of the QSD2 approximation with 100,000 particles in a double well Bose-Hubbard Model of a BEC with encouraging results, and also contains a summary and conclusions.

2 Quantum State Diffusion: Outline of the Formalism

Quantum State Diffusion (QSD) [28] is a stochastic, or Brownian quantum random walk, technique for solving problems which may be described using a density-matrix formulation of the interaction between a quantum system and a measuring apparatus. Rather than working directly with the density matrix, QSD begins with a wave function, $|\psi>$. The wave function dynamics are controlled by a Hamiltonian H and coupled to the outside world by operators representing "measurements" being made on the system or other interactions with the environment. These operators may even include spontaneous decay of the system. We might identify each realization of the trajectory of such a wavefunction as representing a single measurement. Averages follow from collection of data over many such trajectories, just as in the laboratory where average values are slowly accumulated. The emergence of interference, particle by particle, as in the work of Tonomura *et al.* [39], is an excellent example of this process. The effects of measurements, and other interactions, on the initial wavefunction are mathematically described via appropriate *Lindblad*

operators. For example, a harmonic oscillator with Hamiltonian $H = a^\dagger a$ with eigenvalues $0, 1, 2, 3, \ldots, N, \ldots$ and corresponding Fock space eigenfunctions $|N>$, where $H|N>= N|N>$, might be subject to measurements of its quantum state "N" via a measurement Lindblad $L_N = S\ a^\dagger a$, where "S" represents the strength of the measurement, while at the same time being subject to decay via the Lindblad $L_D = D\ a$, with a decay rate determined by the constant "D." Here a and $a^\dagger$ are the usual Fock lowering (destruction) and raising (creation) operators. This is, further illustrated below, is also considered in some detail by Percival [28] in his textbook encapsulation of the QSD technique.

What is the evolution of an initial state $|M>$ simultaneously subject to the dynamics of the Hamiltonian, responding to external measurement of its state, and undergoing decay? One could solve the evolution of the appropriate density matrix equations, but these are of a dimensionality of the *square* of the dimensionality of the Hilbert space for $|\ \psi>$, and thus are often impractical. The QSD method generates independent *quantum trajectories*, to be illustrated below, whose aggregate statistical properties contain exactly the same information as the solution of the full evolution of the density matrix. The advantage is that each trajectory exists in a space of the same dimensionality as the original Hilbert space, not its square. A natural, although perhaps too anthropomorphic, conceptualization also follows: each quantum trajectory might correspond to a single realization of a quantum measurement. Quantum averages can be obtained from the average of many such trajectories, just as experimental quantum averages correspond to the results of many experiments performed on a series of many independently, but identically, prepared replicas of a quantum system. But, as the evolution of each trajectory can actually be visualized (again, see below), such individual trajectories give a feeling of what might actually be occurring during a quantum measurement, each stochastic time step leading to partial collapse of the wave-function. As data are collected the wavefunction indeed partially collapses, corresponding to our gain in knowledge of its state. It is this effect which is referred to as the back-action. Thus each trajectory seemingly provides a "picture" of what is actually *happening* as a quantum measurement is made. This progress report is not the place to discuss the derivation of the formalism or to properly address questions regarding the correct interpretation of individual QSD trajectories. The interested and motivated reader is pointed to the clear, although perhaps simplified for pedagogical purposes, treatment of QSD by I. C. Percival [28]. Percival not only outlines the theory along its numerical implementations and philosophical consequences, but also gives a thorough introduction to the deeper literature.

We begin with a simple example: suppose we have an oscillator in state "N" and an apparatus which measures the value of "N" (with the output being a dial reading "M", $M = 0, 1, 2, \ldots N \ldots$ etc.). The operator which *reads* N is the Lindblad $L = L_N = Sa^\dagger a$, which in this simple case is proportional to the Hamiltonian for the system. S is the strength of the measurement, i.e., a measure of the coupling of the system to the measuring apparatus.

(Our next example will be more complicated!)

In Section 6 it will be pointed out that as more and more precise measurements of N lead to loss of information about the phase of the system. The particle measuring Lindblad is thus said to be responsible for "phase diffusion" resulting from the quantum back action on the system. Phase diffusion, caused by measuring the "local particle density," can destroy a BEC via phase decoherence. The local phase gradients corresponding to this decoherence create currents, which are equivalent to local heating, taking the condensate above its quantum phase transition temperature. Thus, as is the all too usual case in quantum measurements, more precise knowledge of one quantity leads to increasing uncertainty in its conjugate variable. In the case of measuring the particle number N, this conjugate variable is the phase.

Suppose that our system is initially in state $\mid \psi >$. The measurement apparatus (and H) now "act" for a short time interval dt and $\mid \psi >$ evolves into $\mid \psi > + \mid d\psi >$. Here $\mid d\psi >$ is given by

$$\mid d\psi >= -\frac{i}{\hbar} H \mid \psi > dt - \frac{1}{2}(L - \langle L \rangle)^2 \mid \psi > dt \; + (L - \langle L \rangle) \mid \psi > d\xi \qquad (2.1)$$

The deterministic terms proportional to dt represent the usual Schrödinger time evolution due to the Hamiltonian H and the change induced in $\mid \psi >$ by the fact that the system has been subject to a measurement of "N" for the time interval dt. $< L >$ is the mean value of L with respect to the normalized state $\mid \psi >$. The implicit presence of the wavefunction itself in the term $< L >$ makes the apparently linear Eq. (2.1) highly *non-linear!* The second term in the time evolution is proportional to $d\xi$, and represents quantum stochastic diffusion. It is defined as $d\xi = (\sqrt{dt})e^{i2\pi r}$, where r is a real random number on the interval $(0, 1]$. The stochastic phase factor $e^{i2\pi r}$ thus introduces a random complex phase on the interval $(0, 2\pi]$ and a complex diffusive time element of magnitude $\sqrt{dt}$. The origin, see Percival [28], of the $\sqrt{dt}$ is the quantum analog of the fact that diffusive processes spread with a mean square variance of t, and thus a variance proportional to $\sqrt{dt}$. The quantum analog includes a random phase in this diffusive process. Stated more succinctly, $d\xi$ is a complex random variable such that $<< d\xi >>= 0$ and $<< d\xi^* d\xi >>= dt$, and where $<<>>$ denotes, not the quantum expectation value, but the average over realizations of the random variable $d\xi$. Eq. (2.1) is not fully general, as advantage has been taken of the fact that L is Hermitian in the case that $L = SH$. It does, however, immediately show two important facts, which are fully illustrated in the numerical examples to follow. First, if $\mid \psi >$ is an eigenstate of L, both $(L- < L >)$ and $(L- < L >)^2$ vanish when acting on the state. In an eigenstate, the only time evolution is due to H itself, and the "back action" of measuring the eigenvalue has neither a deterministic nor a stochastic effect on the wave function. This is consistent with the usual *naive quantum measurement theory* idea that measurement of a quantum property gives only eigenvalues of operators associated with that property, and further that once such an eigenvalue is detected the wave

function has "collapsed" (or been "filtered") to give the corresponding eigenfunction. Further measurements then give only repetitions of the identical eigenvalue. Second, and more interestingly: if $\mid \psi >$ is *not* an eigenstate of L, the term $-(((L- < L >)^2)/2)dt$ evolves the system to minimize $(L- < L >)^2$. Namely, it tends to force the system into one of the many possible eigenstates of L. This deterministic tendency is offset by the random diffusive term proportional to the square root of this same term, which is also proportional to $d\xi$. Thus measurement will tend to initiate a diffusive process, with larger diffusive amplitude for larger measurement strength S, whose end result will attempt to produce a zero value of $(L- < L >)^2$. However, the presence of other interactions with the environment may make the dynamics more complex than a simple monotonic decay, as we will see in the following section. This simple example will be crucial to understanding the nature of the decay of Schrödinger Cat states. For these, entanglement produces a value of $< L >$ which is half-way in between initial possible eigenvalues of L for the separate parts of the bipartite superposition. The system is thus fundamentally unstable, and its fluctuating trajectories are inevitably drawn to one of the two collapsed states with equal probability.

Now, in the more general case, [28], there will be many different Lindblads L_k, not all of which are Hermitian. These add linearly, but each with its own random diffusive phase and amplitude $d\xi_k$. Thus the generalization of Eq. (2.1) is

$$\begin{aligned} \mid d\psi >= -\frac{i}{\hbar}H \mid \psi > dt + \sum_j (\left\langle L_j^\dagger \right\rangle L_j - \frac{1}{2}L_j^\dagger L_j - \frac{1}{2}\left\langle L_j^\dagger \right\rangle \langle L_j \rangle) \mid \psi > dt \\ + \sum_j (L_j - \langle L_j \rangle) \mid \psi > d\xi_j \end{aligned} \tag{2.2}$$

In this case the independent random variables $d\xi_k$ must satisfy the independent conditions: $<< d\xi_k >>= 0$, $<< d\xi_k d\xi_j >>= 0$, and $<< d\xi_k^* d\xi_j >>= \delta_{jk}dt$. In practical computations these conditions are met by choosing $d\xi_k = (\sqrt{dt})e^{i2\pi r_k}$, where the r_k are independent random real variables on $(0, 1]$.

3 Quantum State Diffusion: A Simple Application

In Eq. (2.2), as in Eq. (2.1), it is to be noted that the many quantum expectation values $< L_j >$ make the system non-linear. The fact that an expectation value $<>$ requires information about the full state of the whole system implies that pieces of the wave-functions seemingly far away from each other in either coordinate or Fock space may strongly affect one another...this being Einstein's *Spooky Action at a Distance*. Thus the reader is warned to expect, and we will indeed see, the effects of such non-locality. Even though the quantum trajectory may indeed be "observed" step by step as it evolves and diffuses, the essential mystery of the non-locality of quantum mechanics is actually already built into the numerical formalism of QSD. Thus, sadly, one learns nothing about how it works

(or why it exists!) from watching the evolving trajectories. What can be learned is how to control nonlocality and how to formulate experiments needed to observe such strongly non-classical effects.

However, in simple cases where such non-locality does not play a strong role, interpretation of the QSD trajectories is straightforward and gives a useful, robust interpretation of the measurement process. We now consider such an example: the Harmonic Oscillator with the measurement and decay Lindblads of Section (2). To be explicit, let us again consider the harmonic oscillator with Hamiltonian $H = a^\dagger a$ with eigenvalues $0, 1, 2, 3, \ldots, N, \ldots$ and corresponding Fock space eigenfunctions $|N>$, where $H|N>= N|N>$. The oscillator is subject to measurements of its quantum state "N" via a measurement Lindblad $L_N = S\, a^\dagger a$, where "S" represents the strength of the measurement, and at the same time subject to decay via the Lindblad $L_D = D\, a$, with a decay rate determined by the constant "D".

We now solve the stochastic Eq. (2.2) in the subspace of oscillator states with N taking the values $0, 1, \ldots, 6$, with an initial condition $N = 5$, so that initially $< i|\psi >= (0, 0, 0, 0, 0, 1, 0)$. Here we have switched to a vector coefficient representation of $< i|\psi >$ in the basis of number states $i = 0, 1, \ldots, N$, of the single oscillator. With the choice of measuring strength $S = 8$, decay constant $D = 0.9$, and timestep, $dt = 0.00002$, and with a good generator of real random numbers on the interval (0,1], the methods of Section 2 may be implemented using an Euler type integration scheme. At each time step $|\psi> \rightarrow |\psi> + |d\psi>$ via Eq.(2.2) with $L_1 = L_N$, and $L_2 = L_D$, followed by iteration to the next step. The norm of the time evolving complex wave-function is preserved "on average" due to the chosen statistical properties of $d\xi$. Nonetheless, because the Euler method is not stable with respect to non-linearities, it is useful to "renormalize" the wave function on a regular basis. Results of such a computation are shown in Figure (3.1), where $< H >$ for a single QSD trajectory is shown.

Examination of Fig. (3.1) makes it evident that $S = 8$ is a "strong" measurement regime in that the oscillator takes what might be though of as "quantum jumps" between the quantized energy levels, $5, 4, 3 \ldots$ the initial state being $N = 5$, as energy is lost. Between such jumps the measurement Lindblad tends to cause the system to "stick" at or near an "eigenstate" of the observable being measured (in this case the quantum state of the system, as indicated by its quantum number N). From a practical point of view it is the deterministic term $(L- < L >)^2$ in the *measurement Lindblad* which causes this effect; the Hamiltonian H has nothing to do with this sticking of the trajectory near its eigenvalues. The eigenfunctions of H just happen to be the same as those of the Lindblad in this simple case. Perhaps this is surprising at first, yet it is the same as in the situation in the laboratory! The dial or pointer on laboratory apparatus has no insight as to the nature of the quantum Hamiltonian, it just puts data counts in labeled "boxes" whose dynamics and structure are classical, not quantum. Nonetheless, there is a temptation to think of Figure (3.1) as

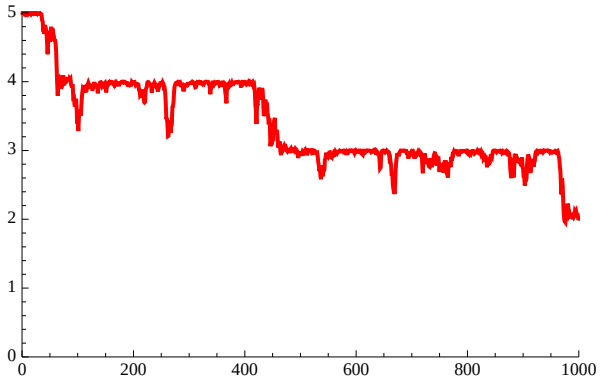

Figure 3.1: Decay of a quantized harmonic oscillator, with energy level spacing one, under the influence of simultaneous observation, ($S = 8$ in this example) and subject to energy loss to an external bath,with coupling $D = 0.9$.

showing the evolution of the oscillator as it loses discrete amounts of energy. Alternately, as in what follows, the system loses *particles* or *quanta* from a system of atoms or photons. In the latter case, N simply counts these particles (or quanta), which are detected by the apparatus. Coupling to this apparatus is here represented by L_N. The abscissa indicates the number of QSD time steps "saved" in the evolution of this free system, the total number of steps actually being 100,000, in the calculations of Figures (3.1)-(3.4). In this, and the following three figures, this amounts to time running from 0 to 2, in units of the natural scale conjugate to energies $0, 1, 2, \ldots$ The system does decay, and different realizations of this process would produce a mean first order decay rate proportional to D^2. While the jumps would occur at different times, a smooth mean exponential decay would result from taking an average over a large ensemble of trajectories. Thus the QSD simulations reconcile the seemingly disparate views of quantum systems making "jumps" between eigenstates, and Fermi's Second Golden Rule with its prediction of exponential decay. This will be exemplified, in a different context, in Section 6.

In all the examples shown, except the last in Section 6, time propagation is carried out with the simple Euler method implied in Eq. (1,2). As the Euler method is notably unstable, the system vector is renormalized to unity at every Euler time step. Renormalization at every 5th or 10th or 100th step would show essentially similar results for the decaying quantum state N. Averaging over many such trajectories gives the correct mean decay rate. The deviation of the norm from unity is shown in Figure (3.2) for each Euler time step over the time scale of Figure (3.1). In this figure the state is manually renormalized every hundredth time step. Were it not renormalized at an appropriate frequency, the Euler computation illustrated would eventually become completely unstable and useful information would not be obtained. Knight *et al.* [31] (also see references therein) have extended the Euler method to allow direct integration of Eq. (2.2) in a more stable manner.

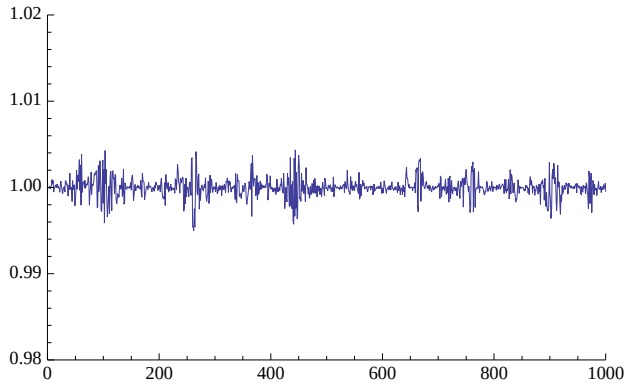

Figure 3.2: In QSD the norm is only preserved "on average." In the data stream shown, the QSD wave-function is allowed to propagate for 100 Euler steps and then renormalized. Normalization is preserved to a few tenths of one percent during these time intervals.

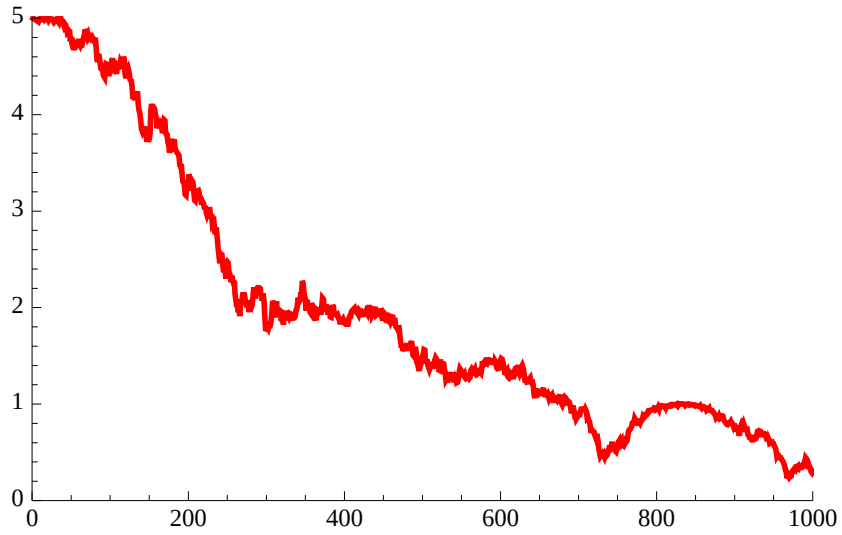

Figure 3.3: Decay of a quantized harmonic oscillator with energy level spacing "one" under the influence of simultaneous observation, as measured by S ($S = 3$ in this example) and subject to energy loss to an external bath, with coupling strength $D = 0.9$.

We now investigate the effects of changing the "measurement strength," S, while holding the decay rate coupling, D, constant. It is evident, see Figure (3.3), that $S = 3$ is a "weaker" measurement regime than the $S = 8$ of Figure (3.1) in that the oscillator still takes what might be thought of, now more impressionistically, as "quantum jumps" between quantized energy levels, $5, 4, 3, 2, \ldots$ as energy is lost, but the energy level spectrum is much less forcefully defined by the measurement and its Lindblad, L_N, than for $S = 8$. In between such jumps the measurement Lindblad still tends to cause the system to occa-

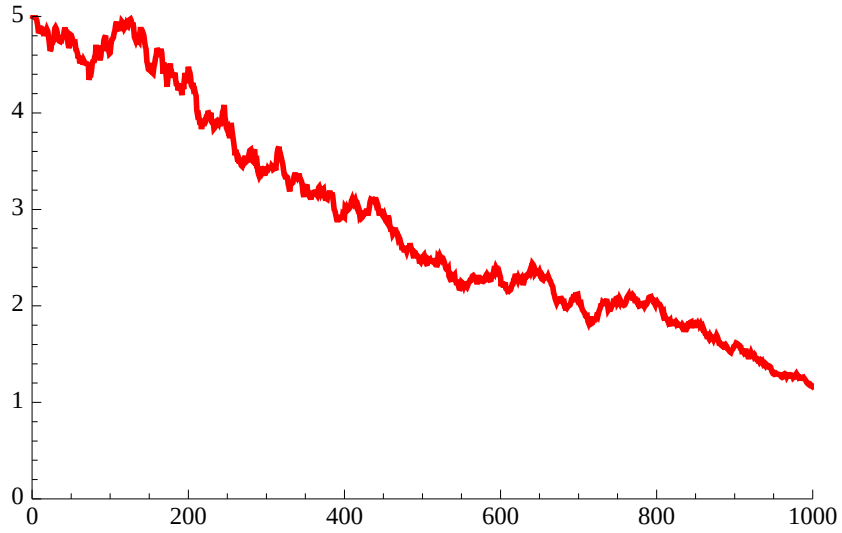

Figure 3.4: Decay of a quantized harmonic oscillator, with energy level spacing "one" under the influence of simultaneous observation, as measured by S ($S = 0.0001$ in this example) and subject to energy loss to an external bath, with coupling strength $D = 0.9$.

sionally "stick" at or near to an "eigenvalue" being measured, but now much less strongly than shown in Figure (3.1). The time scale is again that of Figure (3.1). The time averages of many such trajectories in Figures (3.1) and (3.2) would show essentially the same mean decay rate, as $D$is unchanged. Similar results for very weak coupling are illustrated in Figure (3.4). It is evident that $S = 0.0001$ is a "weak" measurement regime in that the measured oscillator energy simply drifts from higher to lower energy (typically). The energy does not "stick" near any of the eigenvalues, N, which are being observed via the measurement Lindblad. Again, the time scale is that of Figure (3.1). In this regime one is less tempted to think of the apparatus as inducing discrete quantum jumps. Yet, the mean decay profile of an ensemble of QSD trajectories would still yield approximately the same decay rate. The Hamiltonian and decay Lindblads are identical in Figures (3.1), (3.3), and (3.4), strengthening the view that the coupling of the system to the apparatus creates the actual observation.

4 Decay of a Superposition State of a Single Oscillator, and Introduction of a Simple Model

Now we consider the time evolution of a superposition of the single oscillator states discussed in Section 2. The Hamiltonian and Lindblads are precisely the H, L_N and L_D of that section; but now we consider the evolution and measurement of N with initial

normalized single oscillator superposition state $< i|\psi >$ = $(1,0,0,0,0,0,1)/\sqrt{2}$ (again using the vector coefficient representation of $< i|\psi >$ in the basis of number states $i = 0,1,\ldots,N$, of the single oscillator). The measurement strength S is now 0.005, and the decay constant D is 0.2. As $< L_N >$ is now initially 3, rather far from the $N = 0$ or $N = 6$ of the initial state vector, $(L_N - < L_N >)^2 \mid \psi >$ is non-vanishing until the final, fully decayed state $(1,0,0,0,0,0,0)$ is ultimately reached. Additionally, large fluctuations might be expected because $(L_N - < L_N >)^2$ can decrease for either gain or loss of oscillator quanta. The decay of $< L_N >$ is plotted in Figure (4.1). Indeed, large fluctuations are seen, and the value $D = 0.2$ gives a longer decay time than in the earlier examples of decay of the $N = 5$ state shown in Figs. (3.1), (3.3), and (3.4). Note that in the earlier figures, the actual time evolution is over only 2 time units, rather than the 60 shown in Figs. (4.1) and (4.2).

The eventual goal of this progress report is to present a method for working with 10^5 to 10^6 particles or (oscillator quanta, these being interchangeable terms in the Fock space description). Development of simple approximations will thus be useful. Further, in the following Sections 5 and 6 we will wish to work with models of Schrödinger Cat states thought of as "two state" systems: namely with a Fock state $|N,0>$ describing all particles on the left in a double well system (or, equivalently, all excitations in the left oscillator), a fock state $|0,N >$ equivalent to all particles being on the right, or the macroscopic superposition of both: $\mid \psi >$ = $(|N,0> + |0,N >)/\sqrt{2}$. We thus attempt to reproduce, within a two "state model", the data of Figure (4.1), which is, after all, a system with an initial superposition of two states, each with particle numbers far from their mean value.

A two state description (which we refer to as a QSD2 approximation) might at first seem somewhat optimistic, or even completely unrealistic. We therefore test it here in a novel manner. Linear regression of the data of Figure (4.1) gives an effective first order decay constant k_{eff} =0.07596, which fits the data very well at longer times. This indicates that, after initial transients, the mean decay is indeed exponential. Defining $L2$=$L2_N$ as the diagonal 2 by 2 matrix with elements $Ne^{-k_{\text{eff}}t}$, which are retained for $N = 6$ and $N = 0$ only. The initial vector $(1,0,0,0,0,0,1)/\sqrt{2}$ we now truncate to $(1,1)/\sqrt{2}$, keeping only the two non-vanishing initial occupied states, $N = 0$ and $N = 6$. Using the value of k=k_{eff} empirically determined from the full QSD calculation of Figure 5, we now carry out a $2-$dimensional QSD. The decay Lindblad is no longer needed because its effect has been taken into account via the decaying exponentials $Ne^{-k_{\text{eff}}t}$. We now follow the QSD2 evolution equation

$$\mid d\psi >= -\frac{i}{\hbar}H \mid \psi > dt - \frac{1}{2}(L2 - \langle L2\rangle)^2 \mid \psi > dt \; + (L2 - \langle L2\rangle) \mid \psi > d\xi \qquad (4.1)$$

We have now replaced the 6 dimensional Fock space of Figure (4.1) with a two dimensional truncation, using an empirically decaying 6th state $N(= 6\exp(-k_{eff}t))$. The Lindblad describing fluctuations between the two remaining states is retained. Can this

simplification possibly give even a vaguely plausible description of the dynamics? Figure (4.2) indicates that it is, indeed, possible!

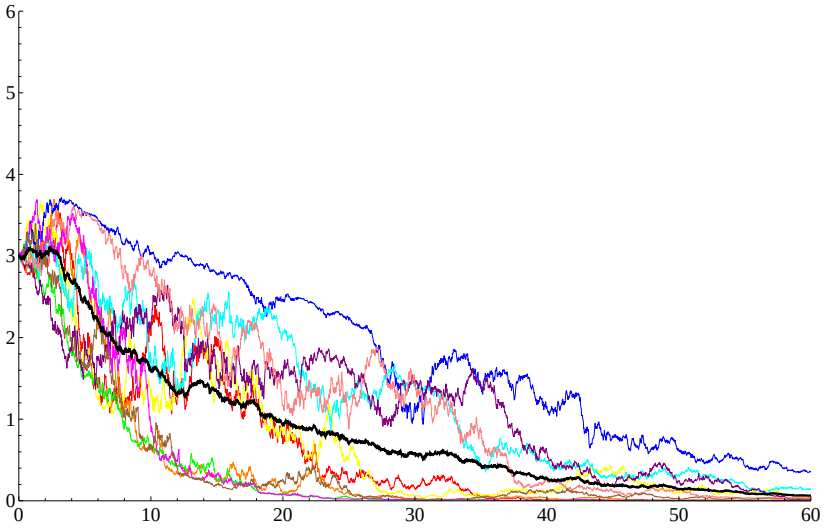

Figure 4.1: $< L_N >$ for ten QSD trajectories (thin lines), and their mean (heavy line), for the initial superposition state, described above, plotted for 60 time units.

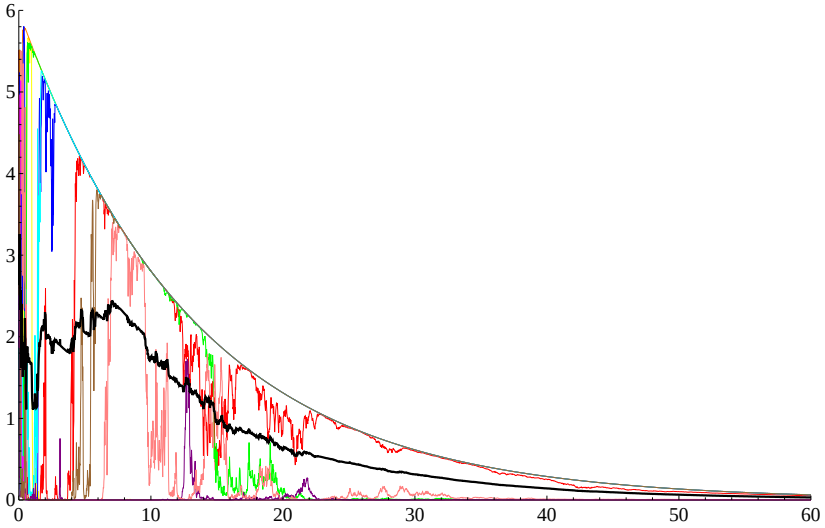

Figure 4.2: Two state modeling of the dynamics leading to the results of Figure (4.1). The results of ten QSD2 trajectories, from Eq. (4.1), for $< L2_N >$, (lighter lines) and their mean (heavy line) are shown.

Comparison of Figures (4.1) and (4.2) clearly indicates that, following initial transients,

the mean values of the oscillator excitation (or particle number) are in quite reasonable agreement, although the QSD2 calculation in its initial form certainly exaggerates the fluctuations. The latter effect is because in QSD2 the fluctuations can only take place between between the $N = 0$ and $N = 6\exp(-k_{eff}t)$ states, whereas fluctuations of this magnitude are not seen in the full QSD dynamics of Figure (4.1). This suggests the need for a renormalization of the fluctuations, which we carry out successfully for the case of the two-oscillator superposition states considered in the following section.

5 Decay of Schrödinger Cat States of Two Independent Quantum Oscillators

Having introduced the QSD model and applied it to a single harmonic oscillator in two very different initial states, we are now ready to study the main objects of our interest, namely number entangled states of two independent oscillators. Or, what is essentially the same problem with the added constraint of number conservation, number entangled states of bosons confined in a double well. See the theoretical work of Khan, Reinhardt and Perry [23, 24, 34] where coherent highly excited states of a BEC in a double well are discussed theoretically. Some of these are also seen experimentally. Namely, Oberthaler *et al.* [1] have observed Josephson oscillations of BECs in a double well system and also the *self-trapped* stationary excited states wherein an excess of particles are trapped in either the Left or Right well. In the latter case, particles do not tunnel even though tunneling would be possible for less highly excited states. These non-linear self-trapped states are of the form of symmetric pairs: $|N-n, n>$ and $|n, N-n>$, with $n << N$. Here the notation $|P, Q>$ indicates $N = P$ in the Left potential well, and $N = Q$ in the Right well. Number conservation for atomic BECs implies $P+Q = N$; however, for the two oscillator problem we will only require $P, Q < N$,, i.e., that each oscillator has maximal excitation N just as in the examples of Sections (3,4). As these self-trapped states are exactly degenerate, we may write the macroscopic superposition states in the form

$$(|N-n, n> +/- |n, N-n>)/\sqrt{2}. \tag{5.1}$$

When $N >> n$, these are referred to as macroscopic superposition states, number entangled states, or (more loosely) as Schrödinger Cat states. We would like to "photograph" them via phase contrast imaging, *a la* Ketterle *et al.* [3]. The $+/-$ linear combinations will be slightly split by tunneling, similar to the splittings observed in superpositions of counter propagating super-conducting loops [13, 41], but such a small energy difference would be difficult to observe in a double well BEC.

Considering the system of two independent and uncoupled oscillators, of the type examined in Sections (3,4) (rather than the number conserving double well BEC itself) as a

model system, we examine the fate of such macroscopic superposition states under observation of the quanta in the Left or Right oscillator. The appropriate Lindblad is $L_N^R = S\ a_R^\dagger a_R$, and the number in the Left well via Lindblad $L_N^L = S\ a_L^\dagger a_L$ where the subscripts L and R on the creation/annihilation operators indicate operators which operate independently in each well. Similarly, there will be independent decay Lindblads, $L_D^L = Da_L$ and $L_D^R = Da_R$ for the Left and Right wells respectively.

As discussed further in section 6, where a more fully realistic BEC example is illustrated, the scattering and absorption of light by atoms are connected via the optical theorem (alternately, the real and imaginary parts of the index of refraction are connected via the Kramers-Krönig relationship). Because particle detection and loss via off-resonant absorption are connected, both must be considered simultaneously. Furthermore, the values of S and D are not independent. In this section we will choose S and D freely for pedagogical clarity. In the first example we take $D = 0.2$, and $S = 0.005$; and in the second, $D = 0.02$, and $S = 0.005$.

Figure (5.1) shows the QSD time evolution of the initial Cat state of the two oscillators $(|6,0> + |0,6>)/\sqrt{2}$ within the full Fock space, i.e., all states $|P,Q>$, such that $P,Q <= 6$. This gives a dimensionality of 49. The coefficients used are $D = 0.2$ and $S = 0.005$. The Hamiltonian term from Eq. (2.2) is simply omitted because its effect is negligible (i.e., we neglect tunneling). The dynamics are then entirely controlled by the four independent Lindblads, and their independent stochastic fluctuations are controlled, in turn, by the four independent sequences of random complex diffusive increments, $d\xi_k$. Normalization of the wave-function then conveys *information* from one oscillator to the other (or, in a BEC, from one part of the condensate to the other) via the entanglement between the otherwise non-interacting oscillators. The is precisely the *spooky action at a distance* of Einstein, Poldoski, and Rosen [32].

As in the case of the superposition state of the single oscillator considered in Section 4, $(|6,0> + |0,6>)/\sqrt{2}$ is not an eigenstate of either L_N^R or L_N^L. Thus $(L- < L >)^2$ will be large and non-vanishing until the system collapses to an eigenstate of L_N^L or L_N^R. The eventual collapse of the state into one well or the other is certain, but occurs unpredictably (with a $50-50$ probability for identical oscillators). All such Cat states are therefore unstable in QSD, just as in nature. What we are attempting to understand and model is the time dependence of this collapse, in order to determine whether phase contrast imaging could detect the initial superposition state before causing it to collapse.

In the presence of decay, the collapsed state will have also lost particles (or excitations of the oscillators), and both effects must be treated simultaneously. The large fluctuations from the average value of 3 particles in each well are easily seen. The fluctuations illustrated run from zero particles on the Left (a fully collapsed state with all remaining excitation belonging to the Right oscillator) up to about 4. Examination of the actual state of the system indicates that after 3 or 4 units of time there are only 4 total quanta of exci-

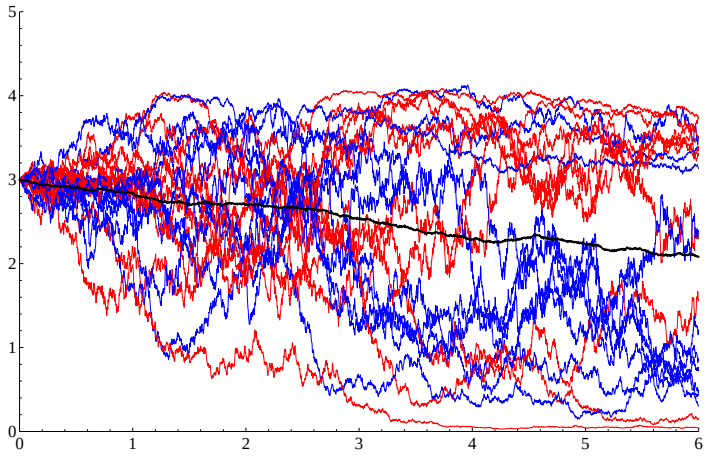

Figure 5.1: Twenty QSD trajectories (with $S = 0.005$ and $D = 0.2$), each starting in the superposition state $(|6,0> + |0,6>)/\sqrt{2}$ and their mean value. What is shown is the number of quanta in each oscillator, namely $< L_N^L >$ and $< L_N^L >$, as a function of time along each QSD trajectory.

tation remaining, so the maximum of "four" indicates a collapse to the Left-localized state $|4,0>$, which then continues to decay.

In the case of two oscillators with the same maximal excitation of $N = 6$, the 49 by 49 stochastic matrix problem is easily solved. This would not be the case were N on the order of 10^5 or 10^6, so approximations must be developed. The effective decay rate corresponding to the data of Figure (5.1), $k_{\text{eff}} = 0.06108$, is used to develop and explore a two state model analogous to that of Section 4. We take the matrix representations of L_N^L and L_N^R to be diagonal, where the diagonal elements are given by $(0, 1, 2, 3 \ldots, N)e^{-k_{\text{eff}}t})$. Each element of the diagonal matrix thus decays with the same rate, obtained from the QSD computation of Figure (5.1). The system is then truncated to a 2 by 2 representation consisting only of the Fock states $|N,0>$ and $|0,N>$; the initial Cat vector becomes $(1,1)/\sqrt{2}$. Again taking $N = 6$ as the maximal excitation of either oscillator, $S = 0.005$, and omitting the Lindblads L_D^L and L_D^R because the effect of decay is now included empirically through k_{eff}, a QSD2 computation is carried out. The results are shown in Figure (5.2).

Examination of Figure (5.2) shows that the decay has been properly captured by the choice of k_{eff}. However, compared to the full QSD data of Figure (5.1), the measurement with strength $S = 0.005$ has resulted in considerably less phase diffusion. The superposition state is thus far more stable with respect to collapse than in the full QSD model. We conclude that both the D and S Lindblads contribute to destruction of the superposition state. In a model containing the D Lindblad only through the empirically determined rate constant k_{eff}, S must be increased to properly model the collapse of the initial superposi-

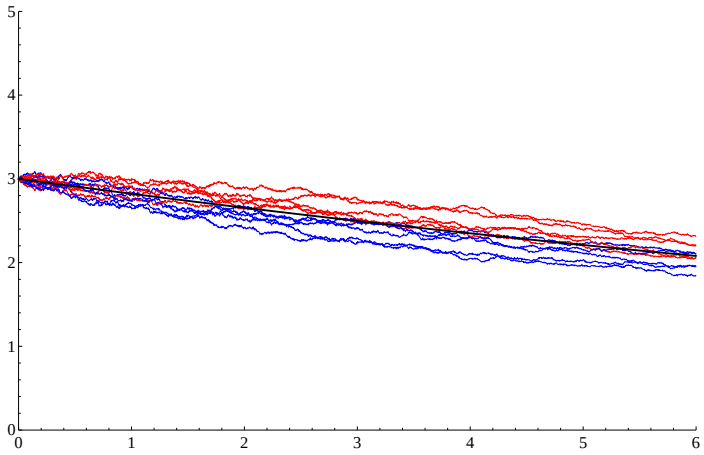

Figure 5.2: QSD2 simulation of the collapse of the superposition state $(|6,0> + |0,6>)/\sqrt{2}$ (with $S = 0.005$ and $D = 0.02$) with the original value of $S = 0.005$. As in Figure (5.1), $< L_N^L >$ and $< L_N^R >$ are shown as a function of time.

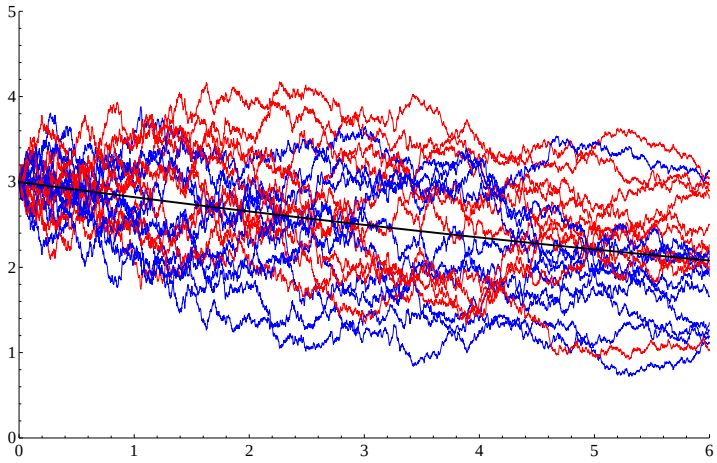

Figure 5.3: QSD2 computation as in Figure (5.2), but with $S = 0.04$.

tion state. This is not surprising. Figures (5.3) and (5.4) show the results of repeating the QSD2 computation of Figure (5.2) with values of $S = 0.04$ and $S = 0.05$ respectively. These two values give decay rates and fluctuations in expectation values of the number operators which nicely bracket the full QSD results of Figure (5.1), indicating that a 2 state model with an empirical decay constant and a "renormalized" measurement strength can accurately reproduce the results of a 49 dimensional computation using a reduced 2 dimensional space. In this case the S value was increased by a factor of 10 to account for the fluctuations absent in the QSD2 computation. We would expect that a smaller value of D,

which leads to slower decay and reduces the importance of the D Lindblad fluctuations, would require a much less dramatic renormalization of S.

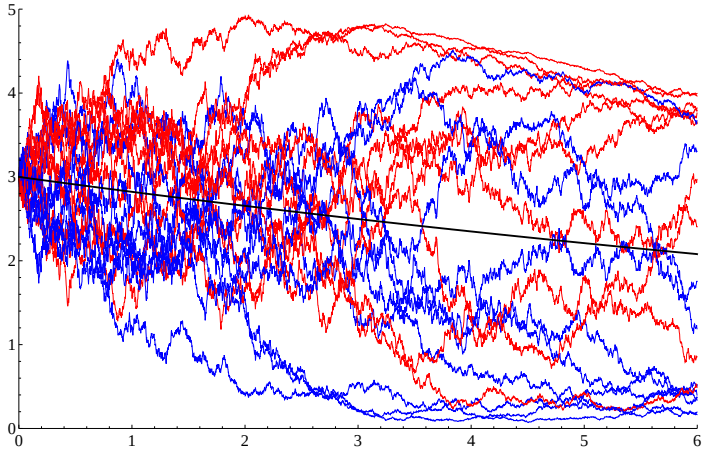

Figure 5.4: QSD2 computation as in Figure (5.2), but with $S = 0.05$. The two values of S in Figures (5.3) and (5.4) exhibit fluctuations with magnitudes that nicely bracket the full QSD results of Figure (5.1).

To check this hypothesis, a full QSD 49 state calculation with the same initial superposition state, but now with $D = 0.02$ (rather than 0.2), was carried out ($S = 0.005$ is unchanged). The results are shown in Figure (5.5).

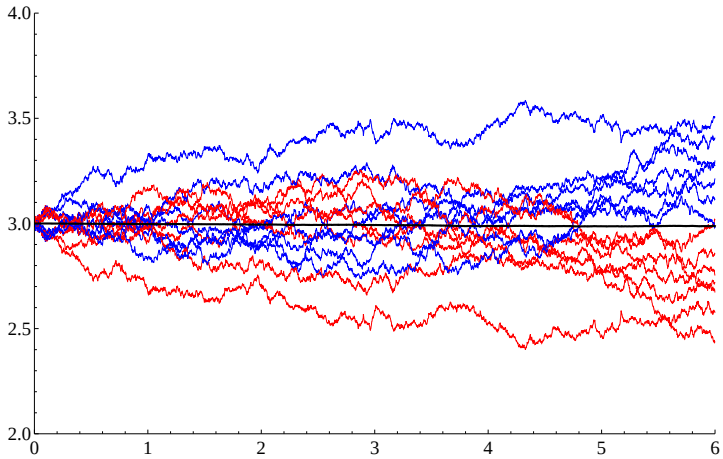

Figure 5.5: Twenty QSD trajectories (with $S = 0.005$ and $D = 0.02$), each starting in the superposition state $(|6,0> + |0,6>)/\sqrt{2}$ and their mean value. What is shown is the number of quanta in each oscillator, $< L_N^L >$ and $< L_N^R >$, as a function of time, along each QSD trajectory.

Figure (5.6) shows the results of a QSD2 computation, as described above, but using

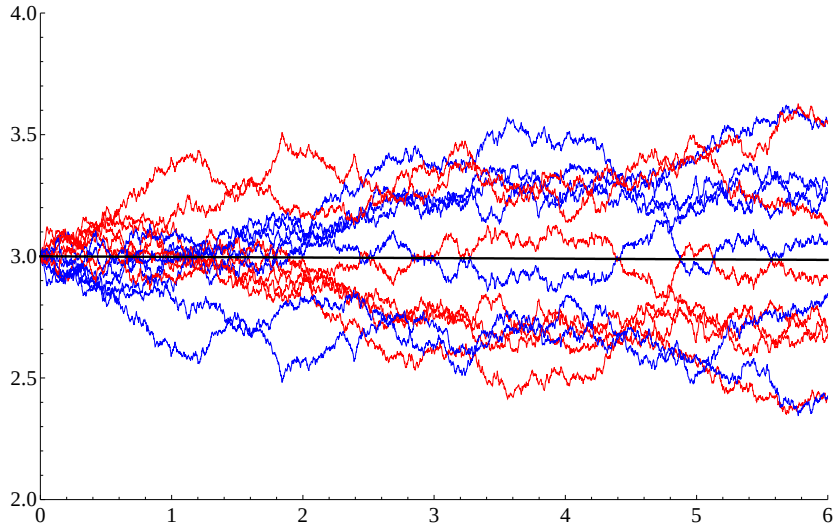

Figure 5.6: QSD2 computation as an approximation to the full QSD simulation of Figure (5.5). Here $D = 0.005$ as in the original simulation.

the original value of $S = 0.005$. This indicates that, for the smaller value of D, the fluctuations induced by the "S" Lindblad indeed dominate and no renormalization of S is necessary to obtain near quantitative agreement between the decay and the rate of collapse during measurement of the superposition state. The state is in fact rather more stable for the smaller value of D.

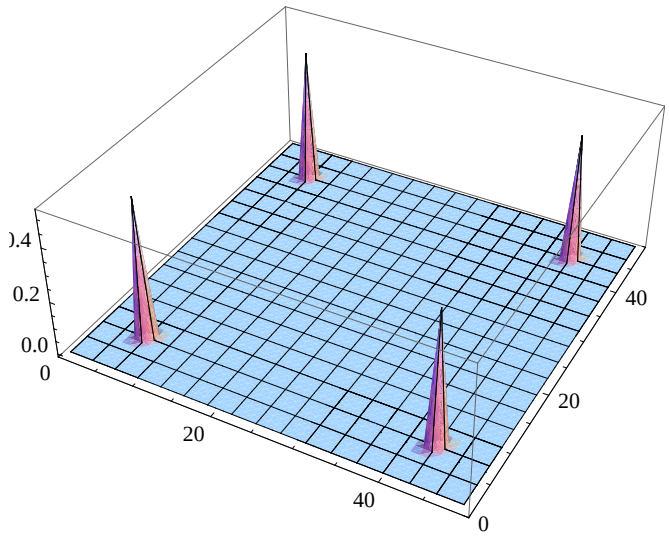

Figure 5.7: Density matrix for a number entangled superposition state at $t = 0$.

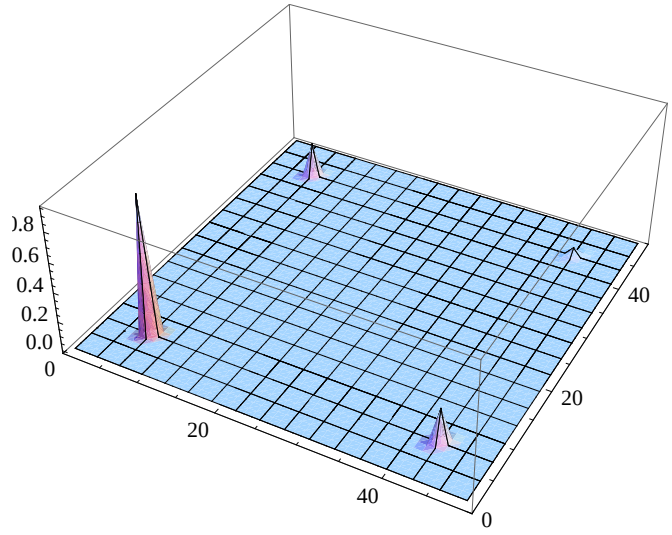

Figure 5.8: Density matrix of a number entangled superposition state at a time half way to full collapse, $t = T/2$. Comparison of Figures (5.7)-(5.9) indicates that collapse of the entangled state is not simply monotonic.

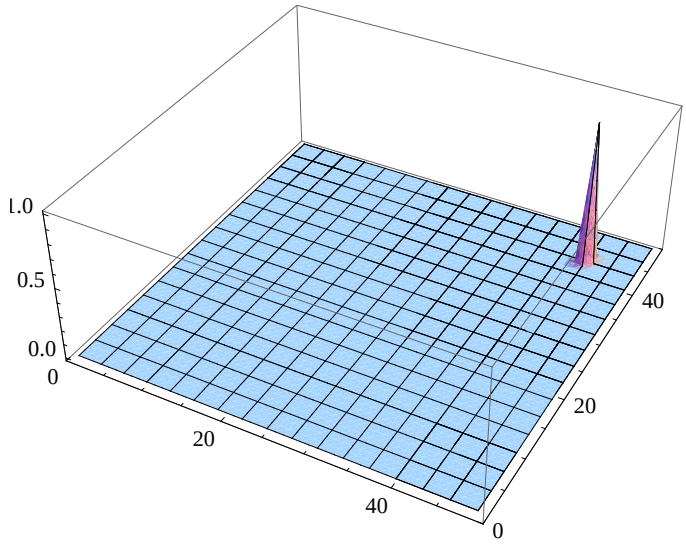

Figure 5.9: Density matrix of of a number entangled superposition state at the time of full collapse, $t = T$.

Another way to visualize the decay of a superposition state such as $(|6, 0 > +|0, 6 >)/\sqrt{2}$ is to examine the time evolution of the density matrix. This is illustrated in Figures (5.7)-(5.9), in which $D = 0.02$ and $S = 1$. This larger value of S gives a very rapid oscillation, followed by decay of the superposition state. The

calculations shown are full QSD computations, but it is evident that a QSD2 2-state model would suffice to reproduce the whole dynamics because the phase diffusional collapse is so rapid that the decay barely plays any role at all. Note the oscillation in population, from the Left to the Right oscillator and back, before the final destruction of the superposition.

6 A More Realistic Application to a Double Well BEC and Conclusions

QSD simulations for the ground state of a double well BEC, where the measurement of the particle number N in either of the wells causes a phase fluctuation of the coherent BEC in that well (simplistically explained by the number-phase uncertainty relationship, $\Delta N \Delta\theta > 1$), have been carried out by Dalvit *et al.* [8]. The resulting phase shift corresponds exactly with the quantum back-action on the system resulting from measuring N to higher precision, thus increasing the phase uncertainty. This phase shift subsequently induces an AC Josephson effect in the double well system, causing particles to flow in a random, oscillatory manner between the two wells. See Figure (3.1) of [8]. Dalvit *et al.* also give estimates of S and D for such a double well system with bosonic Rubidium-87. Note carefully that S and D, as used in the present report, are the square roots of the "phase diffusion" and "spontaneous emission" rates calculated there. Recall also that S and D are not independent, being connected via the optical theorem. An extended discussion of this last point appears in [16, 21, 22], where the explicit relationships are worked out. For a typical Rb BEC, Dalvit *et al.* [8] estimate that $S^2 = 10^{-6}$ and $D^2 = 10^{-5}$. They then correctly argue that for large N, 10^5 or 10^6, phase diffusion dominates because the measurement and decay Lindblads scale as N and $\sqrt{N}$, respectively. Thus, even though the decay rate constant is typically larger than the phase diffusion rate constant, phase diffusion effects actually dominate the solution of Eq. (2.2) when the scaling of the Lindblads with respect to N is included. This suggests that a QSD2 model may well suffice, even though hundreds to thousands of particles may be lost via spontaneous emission if the initial N is on the order of 10^5 (Ketterle estimates that 0.1% to 1% of the particles are lost in a single phase contrast imaging "shot" [3]). The validity of such an approximation is further supported by the results shown in Figures (4.1), (4.2), (5.1)-(5.4), where the rate of quenching for a superposition state, albeit with $N = 6$, not $N = 10^5$, is seen to be modeled well by the QSD2 approximation. Even though many particles are lost, mean decay rates and fluctuation behavior of the superposition states are seen to be well modeled.

Figure (6.1) shows such fluctuations in a preliminary calculation of the QSD2 time evolution for the state $(|N-n, n> + |n, N-n>)/\sqrt{2}$, subject to the "$S$" Lindblad and with the empirical decay mechanism of the QSD2 method, for $N = 10^5$ and $n = 10^4$ over a time interval of 0.75μs. Physically plausible values of S and D are used, as in, for example, [8]. It is clear that experimental observation is at least a possibility, as the phase contrast

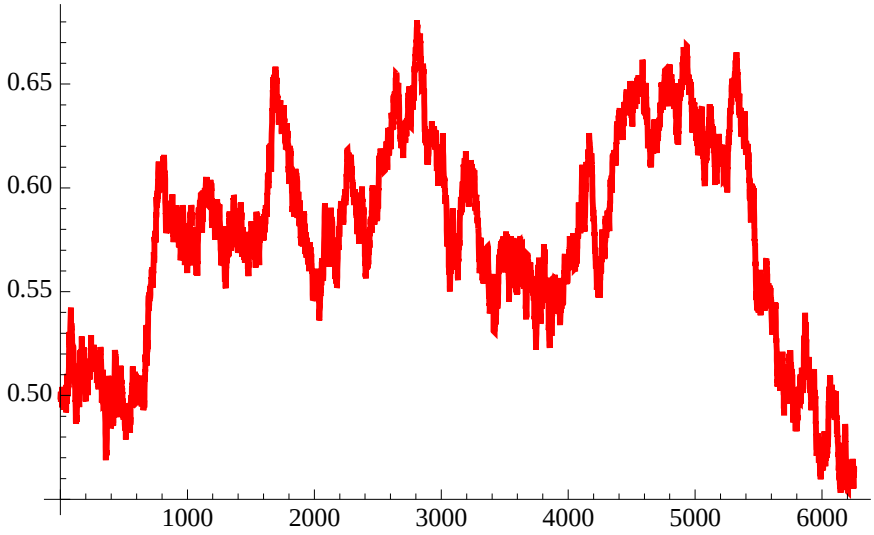

Figure 6.1: QSD2 time evolution of the probability $|c_L(t)|^2$, in the normalized two-state expansion $c_L(t)|N-n, n> + c_R(t)|n, N-n>$, indicating that over a time of 0.75 μs that phase diffusion back-action has not destroyed the macroscopic superposition state. Here $N = 100,000$ and $n = 10,000$, so phase contrast imaging, capturing 100,000 particles in two places at once, is thus a possibility.

microscopy of [3] takes place on a time scale of 1 μs. The key information conveyed in Figure (6.1) is that on the time-scale of 1 μs the superposition state is not quenched. This single QSD2 trajectory is typical for these values of S and N and for this time-scale of observation. Thus phase contrast images showing the bulk of the condensate to be in both wells *at the same time* should be possible. The value of S used in the simulation of Figure (6.1) is, however, an order of magnitude smaller than that of [8]; such experiments will indeed be challenging.

In summary, Quantum State Diffusion has been shown to allow simulation of the time dependent behavior of a double well gaseous BEC during the quenching of a microscopic ($N = 6$) or a macroscopic ($N = 100,000$) superposition state (Schrödinger Cat). Further, as the particle measurement Lindblad (the "S" Lindblad) dominates for large N, it is phase diffusion, rather than particle loss, that kills the Cat. This being the case, particle loss may be handled empirically using the newly introduced QSD2 2-state approximation, making applications to large N systems possible. Preliminary application to a system with $N = 100,000$ indicates that imaging of a macroscopic superposition state in two spatially separate potential wells *at once* is within the realm of experimental possibility.

Acknowledgments

The authors express gratitude to the Saudi Physical Society for support to attend SPS4 in Riyadh, KSA.

References

[1] M. Albiez, R. Gati, J. Folling, S. Hunsmann, M. Cristiani, and M. K. Oberthaler, Direct observation of tunneling and nonlinear self-trapping in a single bosonic Josephson junction, *Phys. Rev. Letts.* **95** (2005), 010402 1–4.

[2] M. H. Anderson, J. R. Ensher, M. R. Matthews, C. E. Wieman, and E. A. Cornell, Observation of Bose-Einstein Condensation in a Dilute Atomic Vapor, **Science 269** (1995), 198–201.

[3] M. R. Andrews, M.-O. Mewes, N. van Druten, D. Durfee, D. Kurn, and W. Ketterle, Direct, Nondestructive Observation of a Bose Condensate, *Science* **273** (1996), 84–87.

[4] M. R. Andrew, C. G. Townsend, H.-J. Miesner, D. S. Durfee, D. M. Kurn, and W. Ketterle, Obervation of Interference Between Two Bose Condensates, *Science* **275** (1997), 637–641.

[5] J. S. Bell, *The Speakable and Unspeakable in Qunatum Mechanis*, Cambridge University Press, Cambridge UK, 1987.

[6] D. Bohm and B. J. Hiley, *The Undivided Universe, An Ontological Interpretation of Quantum Theory*, Routledge, London EC4P 4EE UK, 1993.

[7] N. Bohr, Can quantum mechanical description of reality be considered complere? *The Physical Review* **48** (1935), 696–702.

[8] D. A. R. Dalvit, J. Dziarmaga, and R. Orofino, Continuous quantum measurement of a Bose condensate: A stochastic Gross-Pitaevskii equation, *Physical Review A* **65** (2002), 053694 1–12.

[9] J. Denschlag, J. E. Simsarian, D. L. Feder, C. W. Clark, L. A. Collins, J. Cubizolles, L. Deng, E. W. Hagley, K. Helmerson, W. P. Reinhardt, S. L. Rolston, B. I. Schneider, and W. D. Phillips, Generating Solitons by Phase Engineering of a Bose-Einstein Condensate, *Science* **287** (2000), 97–101.

[10] R. P. Feynman, *Feynman Lectures on Computation*, Westview Press, Boulder, CO, U.S.A. 1999.

[11] C. J. Foot, *Atomic Physics*, Oxford University Press, Oxford, UK, 2005.

[12] G. R. Fowles, *Introduction to Modern Optics*, Holt Rinehart Winston, New York, NY, 1968

[13] J. R. Friedman, V. Patel, W. Chen, S. K. Tolpygo, and J. E. Lukens, Quantum superposition of distinct macroscopic states, *Nature* **406** (2000), 43–46.

[14] G. C. Ghirardi, A. Rimini, and T. Weber, Unified Dynamics for Microscopic and Macroscopic Systems, *Physical Review D* **34** (1986), 470–491.

[15] D. S. Jin, J. R. Ensher, M. R. Matthews, C. E. Wieman, and E. A. Cornell, Collective Excitations of a Bose-Einstein Condensate in a Dilute Gas, *Phys. Rev. Letts.* **77** (1996), 420–423.

[16] W. Ketterle, Quantum backaction of optical observations on Bose-Einstein condensates by U. Leonhardt, T. Kiss, and P. Piwnicki, *Eur. Phys. D* **12** (2000), 123.

[17] W. Ketterle, D. S. Durfee, and D. M. Stamper-Kurn, Making, Probing and Understanding Bose-Einstein Condednsates, in: volume CXL of *Proc. Int. School of Physics "Enrico Fermi"*, 67–176, IOS Press Amsterdam, 1999.

[18] A. J. Leggett, Testing the limits of quantum mechanics: motivation, state of play, prospects, *J. Phys.: Condensed Matter* **14** (2002), R415–R451.

[19] A. J. Leggett, Bose-Einstein Condensation in the Alkali Gases: Some Fundamental Concepts, *Rev. Mod. Phys.* **73** (2001), 307–356.

[20] A. J. Leggett, *Quantum Liquids*, Cambridge University Press, Cambrdige, UK, 2007.

[21] U. Leonhard, T. Kiss, and P. Piwnicki, *Eur. Phys. D* **7** (1999), 413.

[22] U. Leonhard, T. Kiss, and P. Piwnicki, Quantum backaction of optical observations on Bose-Einstein condensates, *Eur. Phys. D* **12** (2000), 124.

[23] K. Mahmud, H. Perry, and W. P. Reinhardt, Phase engineering of controlled entangled number states in a single component Bose-Einstein condensate in a double well, *J. Phys. B (Atomic Molecular Optical)* **36** (2003), L265–L272.

[24] K. Mahmud, H. Perry, and W. P. Reinhardt, Phase control of dynamics in double well BECs: Production of Macroscopic Superposition States, *Phys. Rev. A* **71** (2005), 023615 1–17.

[25] M. A. Nielsen and I. L. Chuang, *Quantum Computation and Quantum Information*, Cambridge University Press, Cambridge, UK, 2000.

[26] R. Omnes, *Understanding Quantum Mechanics*, Princeton University Press, Princeton, NJ, 1999.

[27] R. Penrose, *The Road to Reality*, Alfred A. Knopf, New York, NY, 2005.

[28] I. C. Percival, *Quantum State Diffusion*, Cambridge University Press, Cambridge UK, 1998.

[29] L. Pitaevskii and S. Stringari, *Bose-Einstein Condensation*, Oxford Science Publications, Oxford, UK, 2003.

[30] C. J. Pethick and H. Smith, *Bose-Einstein Condensation in Dilute Gases, 2nd Ed.*, Cambridge University Press,Cambridge, UK, 2008.

[31] M. B. Plenio and P. L. Knight, The quantum-jump approach to dissipative dynamics in quantum optics, *Rev. Mod. Phys.* **70** (1998), 101–144.

[32] B. Podolesky, A. Einstein, and N. Rosen, Can quantum mechanical description of reality be consiered complere? *Physical Review* **47** (1935), 777–780.

[33] W. P. Reinhardt and C. W. Clark, Soliton Dynamics in the Collisions of Bose-Einstein Condensates: an Analog of the Josephson Effect, *J. Phys. B (Atomic Molecular Optical)* **30** (1997), L785–L789.

[34] W. P. Reinhardt and H. Perry, Molecular Orbital Theory of the Bose-Einstein Condensate: Natural Orbitals, Occupation Numbers, and Macroscopic Quantum Superposition States, in: Fundamental World of Quantum Chemistry: A Tribute Volume to the Memory of Per-Olov Löwdin, E. J. Brändas and E. S. Kryachko (EDS), Volume 2, Chapter 12, 305–348, Kluwer, Dordrecht, 2003.

[35] M. Schlosshauer, *Decoherence and the Quantum-to-Classical Transformaton*, Springer, New York, 2007.

[36] E. Schrödinger, Die gegenwertig situation in der quantummechanik, *Naturwissenschften* **23** (1935), 807–849.

[37] Y. Shin, M. Saba, T. Pasquini, W. Ketterle, D. E. Pritchard, and A. E. Leanhardt, Atom interferometry with Bose-Einstein condensates in a double well potential, *Phys. Rev. Letts.* **92** (2004), 050405 1–4.

[38] D. R. Tilly and J. Tilly, *Superfluidity and Superconductivity*, IOPP, Bristol, UK, 1994.

[39] A. Tonomura, J. Endo, T. Kawasaki, H. Ezawa, Demonstration of Single Electron Buildup of Interference Pattern, *American J. Physics* **57** (1989), 117–120.

[40] J. D. Trimmer, The present situation in quantum mechanics: A translation of Schrödinger's cat paradox paper, *Proc. Am. Phil. Soc.* **124** (1980), 323–338.

[41] C. H. van der Wal, A. C. J. ter Haar, F. K. Wilhelm, R. N. Schouten, C. J. P. M. Harmans, T. P. Orlando, S. Lloyd, and J. E. Mooij, Quantum Superposition of Macroscopic Persistent-Current States, *Science* **290** (2000), 773–777.

[42] A. Weller, J. P. Ronzheimer, C. Gross, J. Esteve, M. K. Oberthaler, D. J. Frantzeskakis, G. Theocharis, and P. G. Kevrekidis, Experimental Observation of Oscillating and Interacting Matter Wave Dark Solitons, *Phys. Rev. Letts.* **101** (2008), 130401 1–4.